METHODS OF BIOCHEMICAL ANALYSIS

Edited by **DAVID GLICK**

Life Sciences Division
Stanford Research Institute
Menlo Park, California

VOLUME 25

An Interscience® Publication
JOHN WILEY & SONS, New York · Chichester · Brisbane · Toronto

METHODS OF BIOCHEMICAL ANALYSIS

Volume 25

Advisory Board

N. G. ANDERSON, *Division of Biological and Medical Research, Argonne National Laboratories, Illinois*

TH. BUCHER, *Institute of Physiological Chemistry, and Physical Biochemistry and Cell Biology, University of Munich, West Germany*

W. E. COHN, *Oak Ridge National Laboratory, Tennessee*

P. DOUZOU, *Institute of Physico-Chemical Biology, Edmond de Rothschild Foundation, Paris, France*

R. W. ESTABROOK, *Department of Biochemistry, Southwestern Medical School, Dallas, Texas*

S. GATT, *Department of Biochemistry, Hebrew University-Hadassah Medical School, Jerusalem, Israel*

I. C. GUNSALUS, *Department of Biochemistry, University of Illinois, Urbana, Illinois*

H. A. O. HILL, *Department of Inorganic Chemistry, University of Oxford, England*

J. K. N. JONES, *Department of Organic Chemistry, Queen's University, Kingston, Ontario*

J. H. R. KÄGI, *Biochemical Institute, University of Zurich, Switzerland*

B. G. MALMSTRÖM, *Department of Biochemistry, University of Göteborg, Sweden*

A. MEISTER, *Department of Biochemistry, Cornell Medical College, New York, New York*

R. S. MELVILLE, *National Institute of General Medical Sciences, NIH, USPHS, Bethesda, Maryland*

M. OTTESEN, *Carlsberg Laboratory, Copenhagen, Valby, Denmark*

YU. A. OVCHINNIKOV, *Shemyakin Institute for Chemistry of Natural Products, USSR Academy of Sciences, Moscow, USSR*

J. E. SCOTT, *Department of Medical Biochemistry, University of Manchester, England*

E. C. SLATER, *Laboratory of Biochemistry, B. C. P. Jansen Institute, University of Amsterdam, The Netherlands*

B. L. VALLEE, *Biophysics Research Laboratory, Department of Biological Chemistry, Harvard Medical School, Boston, Massachusetts*

K. YAGI, *Institute of Biochemistry, University of Nagoya Medical School, Japan*

METHODS OF BIOCHEMICAL ANALYSIS

Edited by DAVID GLICK
Life Sciences Division
Stanford Research Institute
Menlo Park, California

VOLUME 25

An Interscience® Publication
JOHN WILEY & SONS, New York · Chichester · Brisbane · Toronto

An Interscience® Publication

Copyright © 1979 by John Wiley & Sons, Inc.

All rights reserved. Published simultaneously in Canada.

Reproduction or translation of any part of this work
beyond that permitted by Sections 107 or 108 of the
1976 United States Copyright Act without the permission
of the copyright owner is unlawful. Requests for
permission or further information should be addressed to
the Permissions Department, John Wiley & Sons, Inc.

Library of Congress Catalogue Card Number: 54–7232
ISBN 0-471-04397-4

Printed in the United States of America

10 9 8 7 6 5 4 3 2 1

PUBLISHER'S NOTE

From its inception in 1940, the Interscience publishing program emphasized the issuance of "Advances" series and the publication of books and series devoted to techniques and methods. It was natural, therefore, to invite David Glick, after publication of his *Techniques of Histo- and Cytochemistry* in 1949, to start *Methods of Biochemical Analysis.* The first volume appeared in 1954. This series has represented a fortunate combination of two of our editorial aims.

The 25-year history of the series has shown that we could not have made a better choice for its editor. Dr. Glick's own field of scientific endeavor, histo- and cytochemistry, was a focal point of biological, chemical, and physical methodology. In addition, he developed a special interest in all phases of methods and techniques applicable to the study of biochemical and biological problems and their instrumentation. In addition, he was able to publish many "firsts" in the methodology that introduced their application throughout the international scientific community.

His travels in Europe, with bases at Carlsberg Laboratory (Copenhagen), Karolinska Institute (Stockholm), and Stazione Zoologica (Naples) were especially devoted to the in-depth study of new developments of methodology. The connections he established there are reflected in the broad international flavor of the Advisory Board and the contributors to the series.

With the publication of the twenty-fifth volume of *Methods of Biochemical Analysis*, we welcome the opportunity to express our gratitude to Dr. David Glick for the splendid editorial guidance he has provided and look forward to many more volumes under his leadership. The long-standing acceptance of the series by life scientists is itself a tribute to his unerring judgment in the selection of topics at the frontiers of biochemical research. Thus Volume 1, published in 1954, had a chapter on luminescence assay and in Volume 24 field desorption mass spectrometry is reviewed. The current volume maintains the high standard for which the series is well known.

Special comment must be made on the international character of *Methods of Biochemical Analysis* as evidenced by the membership of the Advisory Board and the worldwide representation of the contributing authors.

If I may add a personal note, I am particularly honored to have been associated with Dr. Glick over these many years. It has been a relationship of continuing professional and personal gratification.

ERIC S. PROSKAUER

CONTENTS

The Application of High Resolution Nuclear Magnetic Resonance to Biological Systems. *By I. D. Campbell and C. M. Dobson, Department of Biochemistry and Inorganic Chemistry Laboratory, Oxford, England* **1**

Immobilized Enzymes in Biochemical Analysis. *By Johannes Everse and Charles L. Ginsburgh, Department of Biochemistry, Texas Tech University School of Medicine, Lubbock, Texas; Nathan O. Kaplan, Department of Chemistry, University of California at San Diego, La Jolla, California* **135**

Separation and Quantitation of Peptides and Amino Acids in Normal Human Urine. *By Marjorie F. Lou and Paul B. Hamilton, Thomas R. Brown Memorial Research Laboratories, The Alfred I. duPont Institute of the Nemours Foundation, Wilmington, Delaware* **203**

Mapping of Contact Areas in Protein–Nucleic Acid and Protein–Protein Complexes by Differential Chemical Modification. *By Hans Rudolf Bosshard, Biochemisches Institut der Universität, Zürich, Switzerland* .. **273**

Determination of the Activity of Lipoxygenase (Lipoxidase). *By Shlomo Grossman and Rina Zakut, Department of Life Sciences, Bar-Ilan University, Ramat-Gan, Israel* **303**

Author Index **331**

Subject Index **351**

Cumulative Author Index, Volumes 1–25 and Supplemental Volume . **361**

Cumulative Subject Index, Volumes 1–25 and Supplemental Volume . **371**

The Application of High Resolution Nuclear Magnetic Resonance to Biological Systems

I. D. Campbell and C. M. Dobson,* *Department of Biochemistry and Inorganic Chemistry Laboratory, Oxford, England*

I. Introduction 2
II. Basic Concepts 3
  1. The Nuclear Magnetic Resonance Phenomenon 4
  2. The Chemical Shift 6
  3. Spin-Spin Coupling 7
  4. Magnetization and Relaxation 8
    A. Magnetization 8
    B. Spin-Lattice or Longitudinal Relaxation 8
    C. The Bloch Equations and Transverse Magnetization 9
    D. Phase 10
  5. Dipolar Relaxation 11
    A. The Rate Equations and T_1 11
    B. The Transition Probabilities 13
    C. Dipolar Relaxation Effects on T_2 15
    D. The Nuclear Overhauser Effect 16
    E. Generalization of the Dipolar Interaction Equations 17
  6. Chemical Exchange 17
  7. Other Relaxation Mechanisms 19
    A. Scalar 19
    B. Quadrupolar 19
    C. Chemical Shift Anisotropy 20
III. NMR Methods 20
  1. The Magnetic Field B_0 20
  2. Excitation of the Resonances by B_1 23
  3. Detection of the Signals 26
  4. Longitudinal Relaxation 28
  5. Transverse Magnetization 31
  6. Double Resonance 34
  7. ^1H NMR in Aqueous Solutions 38

---

* Present address: Department of Chemistry, Harvard University, Cambridge, Massachusetts.

IV. Resolution and Assignment . . . 41
  1. Resolution of Resonances . . . 41
    A. Linewidths . . . 42
    B. Resonance Overlap . . . 44
    C. Number of Resonances . . . 44
    D. Complex Coupling . . . 51
  2. Measurement of Spectral Parameters. . . . 53
  3. Assignment of Resonances . . . 55
    A. The Spectra of Peptides and Proteins . . . 56
    B. The Spectra of Nucleotides and Nucleic Acids . . . 74
    C. The Spectra of Phospholipids and Membranes . . . 82
    D. The Spectra of Intact Biological Systems . . . 84
V. Applications of High Resolution NMR in Biochemistry . . . 88
  1. Analysis . . . 88
    A. Identification of Compounds . . . 88
    B. Definition of the State of a Given Compound . . . 89
    C. Measurement of Concentrations . . . 90
    D. Measurement of Spatial Parameters . . . 91
  2. Thermodynamics . . . 91
    A. Binding Constants . . . 91
    B. p*K* Values . . . 92
    C. Other Thermodynamic Applications . . . 95
  3. Kinetics . . . 96
    A. Nonequilibrium Measurements . . . 96
    B. Equilibrium Measurements . . . 97
  4. Molecular Structure . . . 102
    A. Quantitative Methods . . . 103
    B. Qualitative Methods . . . 112
    C. Conformational Changes . . . 114
  5. Molecular Motion . . . 115
    A. Proteins . . . 116
    B. Membranes . . . 118
VI. Concluding Remarks . . . 120
Acknowledgments . . . 120
References . . . 121
Appendix A. Mathematical Relationships . . . 128
Appendix B. Solutions of the Chemical Exchange Equations . . . 129
Appendix C. Impulse Response . . . 130
Appendix D. Ligand Binding Equations . . . 130
Appendix E. Correlation of Different Nomenclatures for Aromatic Amino Acids . . . 133

I. INTRODUCTION

Since the last review of nuclear magnetic resonance (NMR) spectroscopy in this series (1), there have been very considerable advances in instrumentation and in methodology. The magnetic field strengths available have increased by a factor of 4, and the sensitivity of instruments has increased by a factor of 40 or more. This has led to a major change in the type of problem that can be tackled by high resolution NMR. For example, detailed studies of macromolecules have become possible, and recently the study of whole tissues (e.g., muscle or bacteria) has begun.

There are a large number of reviews (2–5) and books (6–8) that include the subject of this chapter. Our aim, however, is to cover *methods* suitable for the study of biological systems by high resolution NMR. The application of NMR to specific problems is not reviewed exhaustively. Rather, the examples chosen serve to illustrate the approach to a given problem.

To exploit fully the applications of NMR in biology, it is necessary to make use of sophisticated techniques, as discussed in this chapter both from theoretical and empirical points of view. However we hope that the reader who does not wish to go into detailed theory can omit these sections and still appreciate the biological consequences of NMR.

The theory has been covered in a condensed and somewhat unusual manner. The interested reader should see not only the origin of the rather complex equations that describe some aspects of the NMR phenomenon but also should be able to refer to the theory when reading subsequent sections.

Some of the instrumentation in current use is discussed, particular emphasis being placed on pulse methods. It is the improvement in instrumentation that has, above all, opened the door to the study of a wide range of biochemical problems. However there is also a wide range of different experimental techniques available that can be used in the study of a given system. This chapter discusses methods for increasing resolution and for assignment of the NMR spectra of a variety of systems including proteins, nucleic acids, and whole tissue. It is only when resolved signals in a spectrum can be assigned to specific nuclei in the system that the full specificity of NMR can be exploited.

Finally, some of the applications of NMR in biology are briefly reviewed. These are dealt with under the headings: analysis, thermodynamics, kinetics, structure, and motion. It is our intention to show the scope of NMR in biology by illustrating experimental approaches of different types.

II. BASIC CONCEPTS

This section briefly defines many of the concepts encountered in nuclear magnetic resonance. The material can be read at several levels; a first reading of Sections II.1 to II.4 should give some idea about the fundamental aspects of the method. Sections II.5 to II.7 deal in more detail with aspects that are important in many applications of the technique. Some attempt has been made to indicate how the various equations arise. For the newcomer to the subject it will probably be necessary to use additional material such as refs. 6, 9, and 10. The importance of understanding this subject is that many of the observed phenomena can be treated with rather precise theory in a meaningful way. (In many other forms of spectroscopy, application of sophisticated theory is a less fruitful pastime because of the numerous assumptions involved.)

1. The Nuclear Magnetic Resonance Phenomenon

If a nucleus has a nonzero spin angular momentum $I\hbar$ (integer or half-integer in units of $\hbar$) and a magnetic moment $\boldsymbol{\mu} = \gamma \hbar I$, then an assembly of such nuclei, where γ is the magnetogyric ratio, can exhibit the phenomenon of nuclear magnetic resonance.

The vectors $\boldsymbol{\mu}$ interact with an applied magnetic field B_0 and take up discrete energy values that are labeled by the quantum number m; m can have $2I + 1$ values (e.g., for $I = \frac{1}{2}$, $m = \pm\frac{1}{2}$). Transitions between the m states can be induced by an applied oscillating electromagnetic field. Large numbers of the vectors $\boldsymbol{\mu}$ can be made to change orientation in the field when the resonance condition

$$\omega = 2\pi\nu = \gamma B_0 \qquad [1]$$

is fulfilled. In this equation ω is the angular frequency of the oscillating magnetic field. Such changes in nuclear orientation, when detected, give a nuclear magnetic resonance spectrum.

Many important nuclei possess a spin (see Table I), and each is characterized by a value of γ and I. In some cases, when $I > \frac{1}{2}$, there may also be a quadrupole moment associated with the nucleus (see Section II.5). The

TABLE I

Properties of Some Magnetic Nuclei

Nucleus	Spin (in units of $\hbar$)	Q	Frequency at 10 T (MHz)[a]	Approximate shift range (ppm)[b]	Natural abundance (%)	Relative sensitivity for equal number of nuclei
^{1}H	$\frac{1}{2}$	—	425.8	15	100	1
^{2}H	1	2.8×10^{-3}	65.4	—	1.5×10^{-2}	9.7×10^{-3}
^{13}C	$\frac{1}{2}$	—	107.1	200	1.1	1.6×10^{-2}
^{14}N	1	7×10^{-2}	30.8	—	99.4	1.0×10^{-3}
^{15}N	$-\frac{1}{2}$	—	43.2	400	4	1.0×10^{-3}
^{17}O	$-\frac{5}{2}$	4×10^{-3}	57.6	—	3.7×10^{-2}	2.9×10^{-2}
^{19}F	$\frac{1}{2}$	—	400.1	—	100	0.83
^{23}Na	$\frac{3}{2}$	0.1	112.6	—	100	9.3×10^{-2}
^{31}P	$\frac{1}{2}$	—	172.4	30	100	6.6×10^{-2}
^{35}Cl	$\frac{3}{2}$	8×10^{-2}	41.7	—	75.5	4.7×10^{-3}

[a] The value of γ can be obtained from the formula, $2\pi \times \text{frequency} = \gamma B_0$.

[b] Only quoted for spin $\frac{1}{2}$ nuclei that occur naturally in biological systems. Note that for ^{31}P, biological molecules occur as phosphates; thus the range is only 30 ppm instead of the more usually quoted 600 ppm.

nuclear magnetic resonance, arising from the induced changes in nuclear orientation, is characterized by five parameters: (1) a chemical shift δ, which is a position on an energy scale, measured in hertz (or in parts per million of the applied field) from some suitable standard resonance; (2) a multiplet structure characterized by a spin-spin coupling constant J; (3) a relaxation rate $1/T_2$ related to the linewidth of the resonance; (4) a relaxation rate $1/T_1$, which characterizes the rate at which the resultant magnetization of the spin system returns to equilibrium along the field direction, after a perturbation from equilibrium; and (5) the intensity or the area of the resonance. These parameters are discussed below and are illustrated in Figure 1.

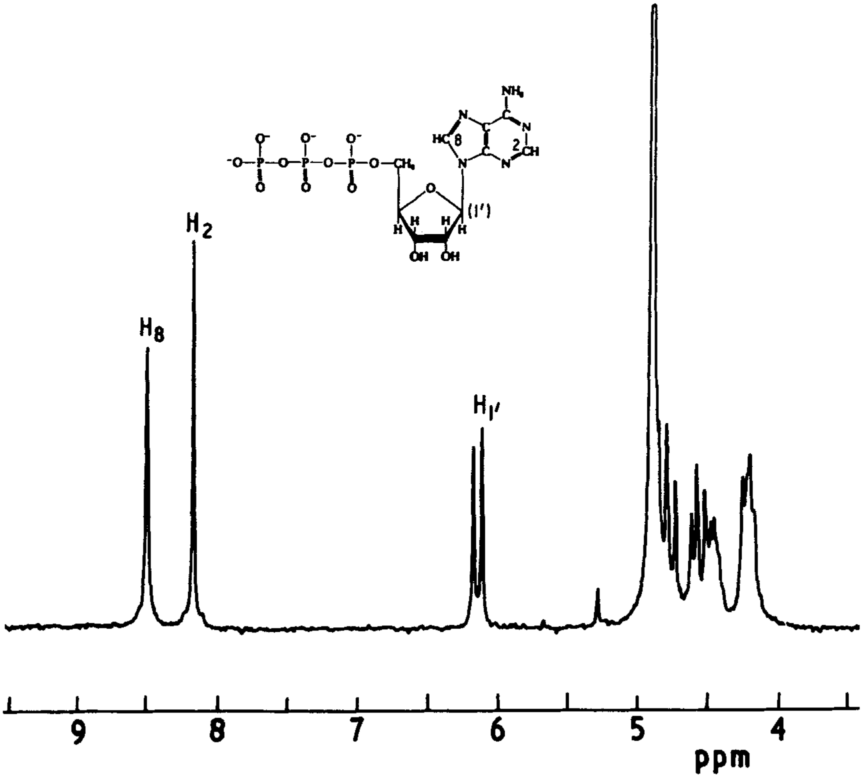

Figure 1. The 90-MHz ^1H NMR spectrum of 30mM adenosine triphosphate in 99.8% D_2O. Each resonance has a characteristic chemical shift value on the horizontal scale and has unit intensity for each proton. The resonances of H_8 and H_2 are singlets but the resonance of H_1' is a doublet because of coupling to the H_2' proton. The linewidths of different resonances (e.g., of H_2 and H_8) are different because of different relaxation times. The resolution and assignment of the remaining protons (H_2' to H_5') is difficult, and this general problem is discussed in Section IV. Note the intense resonance at 4.8 ppm that arises from the residual H_2O in the sample. The removal of solvent resonances is discussed in Section III.7.

2. The Chemical Shift

There are electrons between the nucleus and the applied magnetic field B_0. Currents are set up in the electron cloud which produce a field opposing B_0. Such induced fields are directly proportional to B_0. The dependence of the resonance position on electronic environment depends on the various bonds an atom makes, as well as on the electron distribution. Table I gives the shift range observed for some nuclei. In certain cases a resonance can be assigned to a particular type of atom from its chemical shift position (see Section IV.3). The shifts are also sensitive to changes in the bond structure (e.g., those occurring on protonation). Following the ionization states of particular groups is one of the powerful applications of high resolution NMR (see Section V.2).

In addition to the primary effects listed previously, which depend on the electron distribution around the atom whose nuclear resonance is observed, secondary or through-space effects are very important in biological NMR. Two of these secondary effects can be quantified to some extent, thus giving valuable structural information. These are (*a*) the effect of nearby aromatic rings, and (*b*) the effect of paramagnetic ions.

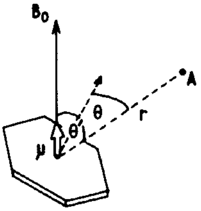

Figure 2. Illustration of ring current shift. The vector of length r joining the center of the aromatic ring and the nucleus A makes an angle θ with the perpendicular to the ring and an angle θ' with the B_0 field direction.

Consider a benzene ring: the π electrons are essentially delocalized, and if B_0 is applied perpendicular to the plane of the molecule, a field that opposes B_0 is produced by the circulating electrons. The field produced may be considered as a dipole $\boldsymbol{\mu}$, which produces a field at a nucleus A, a distance r away (Figure 2). The field at A is proportional to $(3\cos^2\theta' - 1)/r^3$, where θ' is the angle between the B_0 direction and the vector $\mathbf{r}$. In solution the molecule tumbles, and the field at A is averaged over all θ'; but since the induced dipole is very anisotropic (e.g., for a benzene ring $\mu_{//} = 0$), there is a net field experienced at A. This is of the form $(\mu_\perp - \mu_{//})\,(3\cos^2\theta - 1)/3r^3$, where θ is the angle between $\mathbf{r}$ and the perpendicular of the ring. Extensive tables and contour maps have now been constructed for the ring current shifts produced by amino acids and nucleotides (11–13).

The induced shift of a paramagnetic center has the same form as the ring current shifts, although the exact geometric dependence of the shift of the bound metal is less obvious and exchange of the paramagnetic center between different sites can cause complications. Paramagnetic ions especially the lanthanide ions, are a powerful means of determining structure, and these are discussed in Section V.4.

There are various other possible secondary shift effects, which are often very hard to quantify. These include electrostatic effects, the anisotropic shielding of carbonyl groups, and direct overlap of electrons from a paramagnetic center (this effect is often called a contact shift, see Section V.4). Chemical exchange effects are treated separately in Section II.6.

3. Spin-Spin Coupling

The resonances in a high resolution spectrum often exhibit multiplet structure that arises from a weak interaction (of magnitude J Hz) between magnetic nuclei. The interaction is conveyed between the nuclei by the electrons in a chemical bond. The nature of the resulting multiplet depends on the number of bonds between the coupled nuclei, the nature of the bond and on several other factors:

1. The *number* and *spin* of the bonded nuclei causing the fine structure of the resonance. For example, the spectrum of a nucleus coupled to one nucleus with $I = \frac{1}{2}$ is a doublet, whereas the spectrum when coupled to two equivalent nuclei with $I = \frac{1}{2}$ is a triplet with intensities in the ratio 1:2:1.
2. The *chemical shift* δ between the resonance of the observed nucleus and the resonances of the nuclei causing the splitting. When $J \ll \delta$, the spectra are called first order and the two components of a doublet have approximately equal intensity. When J is comparable to δ, the outer components of a pair of doublets are weaker than the inner ones and the spectra are, in general, complex. Computer programs are now available for simulating such spectra, and this aspect is not usually a problem in biological NMR, especially with the use of very high fields (δ increases with B_0, but J is constant).
3. *Bond angles.* The value of J for the ^1H–^1H coupling in a ^1H–X–Y–^1H fragment can be related to the dihedral angle using empirical curves. For example, the observed doublet splittings of the peptide NH resonances of rigid cyclic polypeptides have been related to bond angles (14,15). This method can also be extended to include ^{13}C and ^{15}N couplings.
4. The *populations* of conformers in solution. For example, when three rapidly interconverting rotamers exist in equilibrium, the observed J value is a weighted mean of each of the three possible J values. This is a very important consideration in structure determinations using coupling constants (see Section V.4).

5. The *lifetime* of the nucleus-nucleus configuration within the bond. This period can be short if one of the nuclei has a fast relaxation rate (see Section II.4.B) or if it undergoes rapid chemical exchange. For example, in peptides, the ^{14}N spin-spin coupling is removed because of the fast relaxation rate of the ^{14}N nucleus. Intermediate effects can also be observed when $1/T_1$ the relaxation rate is of the order of J.

6. *Double resonance.* In a manner somewhat analogous to the lifetime effects just described, collapse of multiplicity can be brought about by "stirring" one nuclear spin state with an applied radiofrequency field. This is known as decoupling a resonance (see Section III.6).

The reader is referred to refs. 9 and 10 for further discussion of the appearance of the high resolution spectra of various spin systems.

4. Magnetization and Relaxation

A. MAGNETIZATION

In an applied magnetic field, an assembly of nuclear magnetic moment vectors $\boldsymbol{\mu}$ distribute themselves among the nuclear energy levels according to the Boltzmann distribution law. Because of the small energy separation between the levels, the populations of the states are nearly equal and a linear expansion of the Boltzmann exponential is nearly always valid, as is the application of classical mechanics. In a two-level system, the equilibrium magnetization along the applied magnetic field direction (z) is $M_z^0 = \gamma\hbar(N_2^0 - N_1^0) = \gamma\hbar n_0$, where N_2^0 and N_1^0 are the populations of the levels. We shall see later that M_z^0 is proportional to the maximum observable signal in the NMR experiment, and this means that resonance intensity can be related directly to the number of spins in the sample.

B. SPIN-LATTICE OR LONGITUDINAL RELAXATION

In NMR all the transitions between energy levels are induced by fluctuating fields at appropriate frequencies because other transitions, such as spontaneous emission, have negligible probability. How then is a Boltzmann distribution set up? The answer is that the local field fluctuations are caused by thermal motions of the "lattice" (nuclei or electrons around the nucleus of interest), and since the lattice energy has a Boltzmann distribution, the probabilities of inducing upward and downward NMR transitions are not equal but differ by a factor determined by the Boltzmann law. This can be simply expressed, for a system of two energy levels, as is observed for spin $\frac{1}{2}$ nuclei; if W_{12} and W_{21} are the transition probabilities defined in Figure 3.

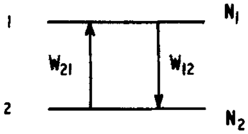

Figure 3. Two energy levels (1 and 2) are shown with populations $\mathcal{N}_1$ and $\mathcal{N}_2$. The probability for the transition 2 → 1 is W_{21} and for 1 → 2 is W_{12}.

The rate equation is

$$\frac{d\mathcal{N}_1}{dt} = \mathcal{N}_2 W_{21} - \mathcal{N}_1 W_{12} \qquad [2]$$

The signal observed is proportional to $M_z = \gamma\hbar n$, where $n = \mathcal{N}_2 - \mathcal{N}_1$, $n_0 = \mathcal{N}_2{}^0 - \mathcal{N}_1{}^0$. At equilibrium $\mathcal{N}_2{}^0/\mathcal{N}_1{}^0 = W_{12}/W_{21}$, and using the relationship $\mathcal{N}_1 + \mathcal{N}_2 = \mathcal{N}_1{}^0 + \mathcal{N}_2{}^0$, the rate equation can be rewritten in terms of n and n_0

$$\frac{dn}{dt} = -(n - n_0)(W_{12} + W_{21}) \qquad [3]$$

This is a simple first-order rate process with rate constant $W_{12} + W_{21} = 1/T_1$, where T_1 is defined to be the relaxation time of the magnetization along the field direction. It is also known as the spin-lattice or longitudinal relaxation time (because it arises from interactions with the surrounding "lattice" and it takes place along the field direction). The solution of [3] is $n = n_0[1 + A\exp(-t/T_1)]$, where A is an integration constant. For example, if at $t = 0$, $n = 0$, $A = -1$, and n recovers from zero to the equilibrium value n_0 at a rate of $1/T_1$. Typical values of T_1 are of the order of 1 sec.

Transitions between energy levels can also be induced by an oscillating radiofrequency field, but now the upward and downward transition probabilities are equal. As a result of this, n tends to zero under the influence of an applied field, a phenomenon known as *saturation* (see Section III,2).

C. THE BLOCH EQUATIONS AND TRANSVERSE MAGNETIZATION

Thus far the discussion has considered only the populations of the energy levels. Since the spin has angular momentum, however, each nuclear moment $\boldsymbol{\mu}$ behaves more like a gyroscope than a bar magnet. In an applied magnetic field, the moments experience a twisting force that makes them precess at a constant angle to the field direction. This means that there may be components of the magnetization at right angles to the field direction. This transverse magnetization is very important, since nearly all the transitions between levels are induced and detected by oscillating fields in this plane. The net magnetization from all the individual nuclei, the bulk magnetization, obeys classical mechanics, and the rate equations for the components of this magnetization in the

x,y-plane are of the form

$$\frac{dM_{x,y}}{dt} = -\frac{M_{x,y}}{T_2}$$

where T_2 defines the decay rate of the x- and y-components of the transverse magnetization.

It is, however, convenient to include in the equation of the transverse magnetization the fact that there is precession at the frequency $\omega_0 = \gamma B_0$ (from [1]) and the effects of an applied rotating field of magnitude B_1 and frequency ω_1. The simplest way of treating this is to view the motion of the bulk magnetization in a new coordinate system rotating at frequency ω_1. The magnetization then behaves as if it were in an effective field $B_0 - \omega_1/\gamma$. When $\omega_1 = \omega_0$, the effective field vanishes. The equations of motion for the components of the magnetization in the transverse plane are now

$$\begin{aligned} \frac{du}{dt} &= (\omega_0 - \omega_1)v - \frac{u}{T_2} \\ \frac{dv}{dt} &= -(\omega_0 - \omega_1)u - \frac{v}{T_2} + \gamma B_1 M_z \end{aligned} \tag{4}$$

where u and v are the components, in the x'- and y'-directions, of the new coordinate system, and B_1 is applied along the rotating x'-axis. These equations simply mean that the effective precession frequency is $\omega_0 - \omega_1$ and that a rotating field B_1 along the x'-direction induces components of M_z into the y'-direction of the rotating frame (see also Section III.2).

Equation [4] together with a version of [3]

$$\frac{dM_z}{dt} = -\frac{M_z - M_0}{T_1} - \gamma B_1 v \tag{5}$$

are collectively known as the Bloch equations, and these equations, with some simple modifications, can be used in nearly all cases to interpret the transient behavior of the nuclear magnetization.

Note that the transverse relaxation time T_2 depends on different processes from T_1 and the two of them are often not equal.

D. PHASE

The directions of the components in the x,y-plane are experimentally observable in NMR. A way of defining the direction of these components is to use a phase angle ϕ (Figure 4*a*). For example, the u and v components are 90° out of phase with respect to each other; components along y' and $-y'$ are 180° out of phase, and so on.

Viewed another way, a solution of [4] is $u = \sin[(\omega_0 - \omega_1)t]\exp(-t/T_2)$, which is an oscillation at frequency $\omega_0 - \omega_1$, which decays with a time

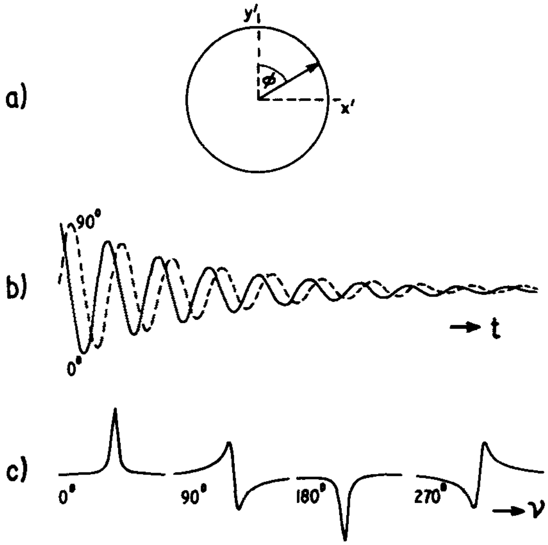

Figure 4. Three representations of the idea of phase in NMR. (*a*) The rotating x', y'-plane, with a magnetization vector that makes a phase angle ϕ with the y'-axis at $t = 0$. (*b*) The signal that would be detected in the x,y-plane as the magnetization vector rotates around the z-axis, for two different values of ϕ. (*c*) The Fourier transformation of signals like those in (*b*) for four different values of ϕ (see also Figures 11, 12, 17 and Section III.5).

constant T_2 (Figure 4). The solution for v, in the absence of B_1, is $v = \cos[(\omega_0 - \omega_1)t]\exp(-t/T_2)$, which is a signal 90° out of phase with respect to the u component.

This concept of *phase* is referred to extensively in Sections III and IV.

5. Dipolar Relaxation

The most important mechanism causing relaxation in solutions of macromolecules is the thermal motion of the molecule, which modulates the local fields produced by the dipole-dipole interactions. The field exerted by one dipole on another has a component proportional to $(3\cos^2\theta - 1)/r^3$, and since molecular motion causes θ to vary, this component fluctuates. Some of the resulting field fluctuations are effective in inducing transitions between the energy levels of the system.

A. THE RATE EQUATIONS AND T_1

Consider two spin $\frac{1}{2}$ nuclei I and S, coupled by dipolar interactions. In general the energy states of I will be influenced by the interaction of S, and

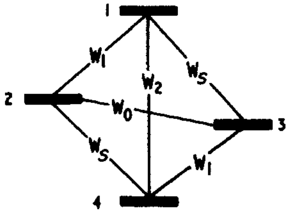

Figure 5. Energy level diagram and transition probabilities for a system of two nuclei, I and S, of spin $\frac{1}{2}$.

vice versa; thus the system is described by four energy levels, as illustrated in Figure 5. The four levels are labeled 1–4 and W_I and W_S are the mean transition probabilities of the principal I and S transitions, corresponding to frequencies ω_I and ω_S, respectively. For dipolar interactions there are two other possible transitions, however, with probabilities W_2 and W_0 with frequencies $\omega_S + \omega_I$ and $\omega_S - \omega_I$. After a perturbation from equilibrium, the rate equations for the populations are of the form (cf. Section II.4.B)

$$\frac{dN_1}{dt} = N_2 W_I + N_3 W_S + N_4 W_2 - N_1(W_I + W_S + W_2)$$

and so on.

The signal observed is proportional to the difference between energy level populations. Defining $n_1 = N_1{}^0 - N_1$, and so on, the rate equations become

$$\frac{d(n_1 - n_2)}{dt} = -(2W_I + W_2 + W_0)(n_1 - n_2) - (W_2 - W_0)(n_1 - n_3)$$

$$\frac{d(n_1 - n_3)}{dt} = -(2W_S + W_2 + W_0)(n_1 - n_3) - (W_2 - W_0)(n_1 - n_2)$$

However $n_1 - n_2 = I_z - I_0$ and $n_1 - n_3 = S_z - S_0$, where I_z and S_z are the components of the bulk magnetization of I and S along the z-direction. Since I_0 and S_0 are the equilibrium magnetization values along z, we have

$$\begin{aligned} \frac{dI_z}{dt} &= -\rho_I(I_z - I_0) - \sigma(S_z - S_0) \\ \frac{dS_z}{dt} &= -\rho_S(S_z - S_0) - \sigma(I_z - I_0) \end{aligned} \qquad [6]$$

where $\rho_i = 2W_i + W_2 + W_0$ and $\sigma = W_2 - W_0$ $(i = I, S)$.

These equations were first derived by Solomon (16). The σ term leads to relaxation behavior described by two exponentials, in general, but in some cases the relaxation can be described by a single exponential with a time constant T_1. This occurs, for example, in the two cases that follow:

1. When $I_z \simeq S_z$ at all times. This case is often observed for two like spins with $\rho_I = \rho_S = \rho$; then

$$\frac{d(I_z + S_z)}{dt} = -(\rho + \sigma)[(I_z + S_z) - (I_0 + S_0)]$$

and

$$\frac{1}{T_1} = \rho + \sigma = 2W_I + 2W_2 \qquad [7]$$

2. When $S_z \simeq S_0$. This case occurs when S relaxes rapidly compared to I (see also case C in Section III.4); then

$$\frac{1}{T_1} = \rho_I = 2W_I + W_2 + W_0 \qquad [8]$$

This equation is very important, since it is applicable to relaxation of a nucleus I by a paramagnetic ion S or when S is subject to selective irradiation.

For further discussions of [6] see Sections II.5, II.6, and III.4. Note that the parameter T_1 is often used even in cases where it does not strictly apply, partly because the errors introduced are often small (17).

B. THE TRANSITION PROBABILITIES

To evaluate the transition probabilities W_I, W_S, W_2, and W_0 for dipolar relaxation, we must resort to quantum mechanics and time-dependent methods involving, for example, density matrices. We merely quote the results here. (see, e.g., refs. 10 and 18).

For *isotropic rotation* of the dipole-dipole pair

$$\begin{aligned} W_I &= \frac{3\alpha}{20} J(\omega_I) \\ W_2 &= \frac{3\alpha}{5} J(\omega_I + \omega_S) \\ W_S &= \frac{3\alpha}{20} J(\omega_S) \\ W_0 &= \frac{\alpha}{10} J(\omega_I - \omega_S) \end{aligned} \qquad [9]$$

where
$$\alpha = \frac{\gamma_S^2 \gamma_I^2 \hbar^2}{r^6}$$

$$J(\omega) = \int_{-\infty}^{\infty} g(\tau) \exp(-i\omega\tau)\, d\tau$$

Here $g(\tau)$ is an autocorrelation function that describes the time scale of the fluctuating magnetic fields. In many cases $g(\tau)$ is exponential and can be expressed as $\exp(-t/\tau_c)$, where τ_c is a correlation time (this simply means that the probability of finding a correlation between the orientation of the dipole-dipole pair, sampled at successively increasing time intervals, decreases exponentially with time constant τ_c). The relationship between $J(\omega)$ and $g(\tau)$ is a Fourier transformation, and when $g(\tau)$ has an exponential form,

$$J(\omega) = \frac{\tau_c}{1 + \omega^2 \tau_c^2} \qquad [10]$$

(see Appendix A and Section III.3, which discusses the Fourier transformation of a decaying NMR signal). When I and S are also coupled by a spin-spin interaction, it is possible to modify these transition probabilities to include this effect (19), but for first-order coupling the result is the same as above.

Very often, especially in macromolecules, the molecular motion causing dipolar relaxation is not simple isotropic rotation, and we consider one simple example of *anisotropic motion.* In the case of the dipole-dipole pair rotating about an axis R, which undergoes isotropic motion at an angle θ to the axis R, the transition probabilities have been calculated by Woessner (20). It turns out that the $J(\omega)$ terms are changed as follows:

$$J(\omega) = \frac{A\tau_R}{1 + \omega^2 \tau_R^2} + \frac{B\tau_B}{1 + \omega^2 \tau_B^2} + \frac{C\tau_C}{1 + \omega^2 \tau_C^2} \qquad [11]$$

where $A = (3 \cos^2 \theta - 1)^2/4$, $B = 3 \cos^2 \theta(1 - \cos^2 \theta)$, and $C = 3(\cos^2 \theta - 1)^2/4$; τ_R is the correlation time of the isotropic motion of R, τ_i is the correlation time of the rotation about R, and

$$\frac{1}{\tau_B} = \frac{1}{\tau_R} + \frac{1}{\tau_i}, \qquad \frac{1}{\tau_C} = \frac{1}{\tau_R} + \frac{4}{\tau_i}$$

This simple model can also give insight into anisotropic molecular motion, which is not strictly of the type described by the model because the transition probabilities are similar in other cases of anisotropic motion. For example, this motion could result from rotation of an ellipsoid (21) or could be concerned with variations in separations between magnetic dipoles (22).

The equations that represent T_1, for relaxation by like spins, are equations [7], [9], [11] evaluated and plotted in Figure 6 for isotropic and anisotropic motion as a function of τ_R.

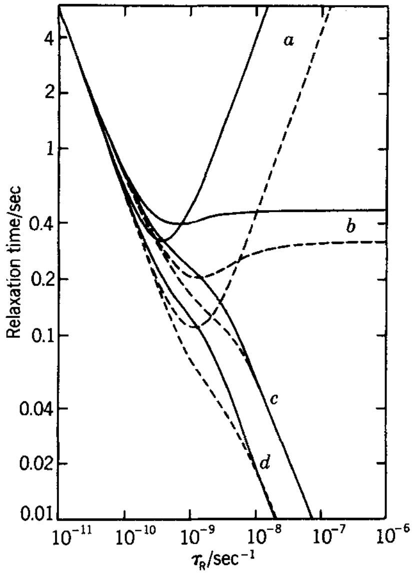

Figure 6. Solutions of [7], [9], [11], and [12] for like spins as a function of τ_R, at 90 MHz (dashed curves) and 270 MHz (solid curves). The α term was calculated by assuming that one proton 2.5 Å away caused the dipolar relaxation. Curves *a* and *c* give the T_1 and T_2 values, respectively, for isotropic rotation. Curves *b* and *d* show the T_1 and T_2 values for anisotropic motion defined by $\tau_i = 10^{-9}$ sec and $\theta = 90°$.

More complex equations for anisotropic motion and dipolar relaxation by translational motion rather than rotation have been published (18,23).

C. DIPOLAR RELAXATION EFFECTS ON T_2

In general the transverse magnetization decays exponentially, unlike the z-axis magnetization. We simply quote the results of calculations by Solomon and others:

$$\text{for like spins:}\quad \frac{1}{T_2} = \frac{\alpha}{2}\,(9W_0 + 10W_I + W_2)$$

$$\text{for unlike spins:}\quad \frac{1}{T_2} = \frac{\alpha}{2}\,(\mathcal{J}(0) + 5W_0 + 10W_I + 20W_S + 5W_2) \qquad [12]$$

For like spins and isotropic rotation, the relaxation equations reduce to the simple forms

$$\frac{1}{T_1} = \frac{1}{T_2} = \frac{3\alpha}{2}\tau_R \qquad \tau_R \ll \omega_I$$

$$\frac{1}{T_1} = \frac{3\alpha}{5\omega^2\tau_R}, \qquad \frac{1}{T_2} = \frac{9}{20}\alpha\tau_R \qquad \tau_R \gg \omega_I$$

Figure 6 also plots [12]; and so on, for isotropic and anisotropic rotation.

D. THE NUCLEAR OVERHAUSER EFFECT

If S_z is driven to zero (saturated) by a selective irradiation at the frequency of the S resonance (see Section III.6), and if I_z is observed under steady-state conditions ($dI_z/dt = 0$) then, from [6] we have

$$\frac{I_z - I_0}{I_0} = \frac{\sigma}{\rho_I} \cdot \frac{S_0}{I_0} = \frac{\sigma}{\rho_I} \cdot \frac{\gamma_S}{\gamma_I} = \eta \qquad [13]$$

where η is defined as the nuclear Overhauser enhancement parameter (24). For example, when $\tau_R \ll \omega_I$, $\sigma/\rho_I = \frac{1}{2}$, thus when $S_0 = I_0$ (like spins) there is a 50% increase in the signal intensity.

Table II lists the values of η for several nuclei for the limits $\tau_R \ll \omega_I$ and $\tau_R \gg \omega_I$ when the S spins are ^{1}H nuclei. Figure 7 plots the variation of η with τ_R for ^{1}H–^{1}H dipolar interaction.

TABLE II

The Nuclear Overhauser Effect[a]

	η	
I	$\tau_R \ll \omega^{-1}$	$\tau_R \gg \omega^{-1}$
^{1}H	+0.50	−1.00
^{13}C	+1.99	+0.15
^{15}N	−3.93	+0.88
^{19}F	+0.53	−1.04
^{31}P	+1.23	+0.002

[a] Where $\rho^* = 0$, S corresponds to ^{1}H, and S is saturated for a time greater than $4/\rho$.

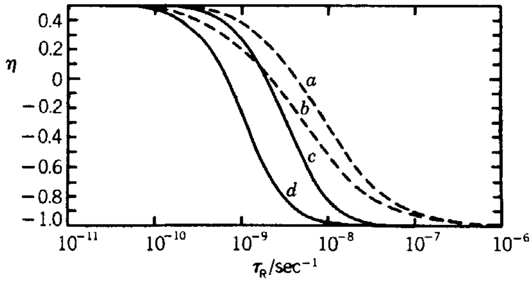

Figure 7. The nuclear Overhauser effect calculated from [7], [9], [11] and [13] for like spins as a function of τ_R. Curves a and b give values of η for anisotropic rotation defined by $\tau_i = 10^{-9}$ sec and θ 90° at 90 and 270 MHz, respectively; curves c and d give values of η for isotropic rotation at 90 and 270 MHz, respectively.

E. GENERALIZATION OF THE DIPOLAR INTERACTION EQUATIONS

When several S-type nuclei (usually protons) cause relaxation of the I spin, the situation is more complex than that outlined earlier, but the various contributions appear to be additive to a good approximation and can be rewritten as $\hbar^2\gamma_I^2\gamma_S^2 \sum_j \bar{r}_j^{-6}$, where $\sum_j$ is a sum over all protons contributing to the relaxation and r_j^{-6} is the mean of the inverse sixth power of the separation between each IS_j pair. The Overhauser enhancement of the I resonance, observed on irradiation of the S spins, however, is not necessarily additive (24).

Other relaxation sources (e.g., dissolved paramagnetic impurities) must also be taken into account. This is done by incorporating additional transition probabilities W_I^* and W_S^* for the I and S transitions (these effects do not change W_2 and W_0). The Overhauser enhancement parameter for a spin pair then becomes

$$\eta = \frac{\gamma_S}{\gamma_I} \cdot \frac{\sigma}{(\rho + \rho^*)} \qquad [14]$$

where $\rho^* = 2W_I^*$.

6. Chemical Exchange

If a nucleus can exist in two or more environments, exchange between these environments may cause very large changes in the observed spectrum and the observed relaxation rates. Consider exchange between two sites with bulk magnetizations I and S, respectively. The effect of exchange between I and S sites on the *longitudinal relaxation* is given by the modified Bloch equation (25)

$$\frac{dI_z}{dt} = -k_I I_z + k_S S_z - \rho_I(I_z - I_0) - \sigma(S_z - S_0) \qquad [15]$$

since magnetization now not only relaxes by a spin-lattice mechanism but there is also a loss from I and a gain from S according to $I \underset{k_S}{\overset{k_I}{\rightleftharpoons}} S$. A similar equation is obtained for dS_z/dt, and this pair of coupled differential equations is similar in many ways to [6], derived for dipolar relaxation. As before, consider the solution of these equations in two special cases.

1. When $I_z \simeq S_z$ at all times (i.e., for like spins),

$$\rho + \sigma = \frac{1}{T_{1I}} = \frac{1}{T_{1S}} \qquad \text{and} \qquad k_S = k_I$$

Then

$$\frac{1}{T_{1_{\text{obs}}}} = \frac{1}{T_{1I}}$$

2. When S_z is constant either by rapid relaxation (e.g., caused by a paramagnetic ion) or by double resonance (see Section III.6); then

$$\frac{1}{T_{1_{\text{obs}}}} = \rho_I + k_I$$

Case 2, which applies when separate resonances are observed for I and S, is known as the *slow exchange* limit. In the *fast exchange* limit an average of the resonance from I and S is observed at all times, and the observed longitudinal relaxation rate is the weighted mean of the relaxation rates $1/T_{1I}$ and $1/T_{1S}$; that is, if f_I and f_S are the fractional populations of the I and S sites, then

$$\frac{1}{T_{\text{obs}}} = \frac{f_I}{T_{1I}} + \frac{f_S}{T_{1S}}$$

In the slow exchange case, since the equations are coupled, irradiation of S can cause changes in the behavior of the I magnetization. For example, the effect of making $S_z = 0$ by double resonance is to change the intensity of I in a manner analogous to the nuclear Overhauser effect. The phenomenon, called *cross-saturation*, is discussed further in Sections III.6 and V.2 and Appendix B.

The *transverse magnetization* rate equations are again obtained by simple modification of the Bloch equations

$$\frac{du_I}{dt} = -\frac{u_I}{T_{2I}} - u_I k_I + u_S k_S - (\omega_I - \omega_1)v_I \qquad [16]$$

$$\frac{dv_I}{dt} = -\frac{v_I}{T_{2I}} - v_I k_I + v_S k_S - (\omega_I - \omega_1)u_I - \gamma B_1 I_z \qquad [17]$$

with similar equations for du_S/dt and dv_S/dt. The general solution of these four coupled differential equations is complex, but they are soluble in certain cases (see Appendices B and D). For example, when the populations of the two sites are equal, the observed T_2 of the averaged resonance (fast exchange) is of the form

$$\frac{1}{T_{2_{\text{obs}}}} = \frac{1}{2T_{2_I}} + \frac{1}{2T_{2_S}} + \frac{\Delta^2\tau}{8} \qquad [18]$$

where τ is the lifetime of each species and Δ is the chemical shift, in hertz, between the I and S environments.

The *chemical shift* observed in the fast exchange limit is a weighted mean of the two environments, that is,

$$\delta_{\text{obs}} = f_I\delta_I + f_S\delta_S$$

where δ_I and δ_S are the chemical shifts of I and S in the absence of exchange ($\delta_I - \delta_S = \Delta$).

Shifts in the slow exchange limit are usually difficult to observe because of line broadening.

7. Other Relaxation Mechanisms

Dipolar relaxation is the most likely relaxation mechanism to be encountered in a biological system, followed by chemical exchange. Other mechanisms must sometimes be considered, however, and we briefly discuss these here. If the various contributions follow exponential rate laws, they can be taken to be additive. For example,

$$\frac{1}{T_{1_{\text{obs}}}} = \frac{1}{T_{1_{\text{dipolar}}}} + \frac{1}{T_{1_{\text{scalar}}}} + \frac{1}{T_{1_{\text{quadrupolar}}}} + \cdots$$

A. SCALAR

This is a mechanism in which the field fluctuations are brought about by fluctuations in the spin-spin coupling. Section II.3 mentioned that if the lifetime of one nucleus is short compared to $1/J$, the multiplet structure of another nuclear resonance collapses. A fluctuating field is still experienced at the other nucleus from this mechanism, and if we define a new correlation time

$$\frac{1}{\tau_e} = \frac{1}{T_{1_s}} + \frac{1}{\tau_h}$$

where T_{1_S} is the relaxation rate of a nucleus (or electron) in the bond and τ_h is the lifetime of the scalar interaction (the lifetime of the bond),

$$\begin{aligned} \frac{1}{T_{1_{\text{scalar}}}} &= \frac{2J^2}{3} S(S+1) \frac{\tau_e}{1+\omega_S{}^2\tau_e{}^2} \\ \frac{1}{T_{2_{\text{scalar}}}} &= \frac{J^2}{3} S(S+1) \left[\tau_e + \frac{\tau_e}{1+\omega_S{}^2\tau_e{}^2}\right] \end{aligned} \qquad [19]$$

These terms are normally small but may be important, especially with paramagnetic transition metal ions such as cobalt. In the case of paramagnetic ions, J is usually replaced by $A/\hbar$ and is called a contact interaction.

B. QUADRUPOLAR

Some nuclei with $I > \frac{1}{2}$ possess an electric quadrupole moment eQ that is the result of the nonspherical nature of the electric charge density. Molecular motion can then cause field fluctuations, hence relaxation. The form of T_1 is similar to the equation for dipolar interactions with α replaced by

$$\left(\frac{e^2qQ}{\hbar}\right)^2 \quad 1 + \frac{\varepsilon^2}{3}\Bigg)$$

where eq is the electric field gradient to which eQ is coupled, ε is a parameter related to the asymmetry around the nucleus.

C. CHEMICAL SHIFT ANISOTROPY

If the chemical shift of a nucleus varies with the applied field direction, molecular motion produces an effective field modulation at the nucleus and gives rise to relaxation. In the case of axial symmetry the equations are of the form

$$\begin{aligned} \frac{1}{T_{1_{\mathrm{csa}}}} &= \frac{1}{15}\gamma^2 B_0{}^2(\sigma_{/\!/} - \sigma_{\perp})^2 J(\omega) \\ \frac{1}{T_{2_{\mathrm{csa}}}} &= \frac{1}{90}\gamma^2 B_0{}^2(\sigma_{/\!/} - \sigma_{\perp})^2[3J(\omega) + 4J(0)] \end{aligned} \qquad [20]$$

where $\sigma_{/\!/} - \sigma_{\perp}$ is a measure of the chemical shift anisotropy (csa). Note that the relaxation, in this case, becomes much more effective at high values of B_0.

III. NMR METHODS

Observation of an NMR signal involves three experimental stages:

1. Application of a magnetic field B_0 to the sample to create an equilibrium nonzero magnetization.
2. Excitation of the spin system by an oscillating radiofrequency field B_1 perpendicular to B_0 (this results in a nonrandom distribution of spins precessing around the field direction and produces components of the magnetization in the x,y-plane).
3. Detection of the components in the x,y-plane.

In addition to the three fundamental points just indicated, data processing methods, multiple resonance techniques, measurement of longitudinal and transverse magnetization, and the special problem of observing ^{1}H spectra in the presence of a large water resonance are briefly discussed.

NMR instrumentation tends to be complex because of the low sensitivity but high information content of the technique. This section outlines some of the sophisticated methods that are available. The aim is always to determine the five parameters defining each resonance (Section II.1). As in many forms of spectroscopy, this can be done by slowly sweeping over the spectrum by changing the excitation frequency. However the efficiency of the collection procedures is very important in NMR hence the emphasis on pulse methods when the parameters of many resonances may be obtained simultaneously.

1. The Magnetic Field B_0

There are two distinct types of magnet in use in high resolution NMR instruments. One is the iron pole piece magnet, which has a maximum field

TABLE III

Factors Affecting Sensitivity[a]

Factor	Dependence
Field strength, B_0	$B_0^{7/4}$
Sample volume, V_s	$V_s^{2/3}$
Time, t	$t^{1/2}$
Temperature, T	T^{-1}
Relaxation times	$(T_2/T_1)^{1/2}$
Nucleus	See Table I
Preamplifier noise figure, F	$F^{1/2}$
Coil geometry	Solenoid ~ 3 times better than Helmholtz
Detector	Quadrature $\sqrt{2}$ times single sideband

[a] Adapted from Hoult and Richards (25). Sensitivity also depends on collection rate, filters, and use of double resonance.

of around 2.5 T,* and the other is a superconducting solenoid, which has a present-day maximum of around 8.5 T. However several groups around the world are actively involved in constructing superconducting systems designed to achieve fields of around 11 T. The aim for higher fields is understandable in terms of the increased sensitivity (Table III), which arises because of a larger energy difference between the energy levels of the system and the increased spread in chemical shift values, which is directly proportional to the applied field.

Both types of magnet need a complex system of additional coils to correct the field homogeneity over the sample to the very high level required (about 1 part in 10^9). These are known as shim coils. To improve further the effective homogeneity, the sample is usually spun about its long axis. This, however, can introduce spinning sidebands, which are related to the spinning frequency and to B_0 and B_1 field inhomogeneities (26).

The field must also have very high long-term and short-term stability . This is achieved by using a completely separate NMR system to *lock* the field. The resonance of a nucleus (usually ^2H), different from the observed nucleus but in the same sample tube, is excited and detected. The field can then be continuously adjusted to maintain the resonance condition $\omega_{\text{lock}} = \gamma_{\text{lock}} B_0$. The lock frequency is usually derived from the same master oscillator as the observing frequency (Figure 8), which leads to very high overall stability (1 part in 10^9).

---

* 1 tesla (T) = 10,000 gauss (G).

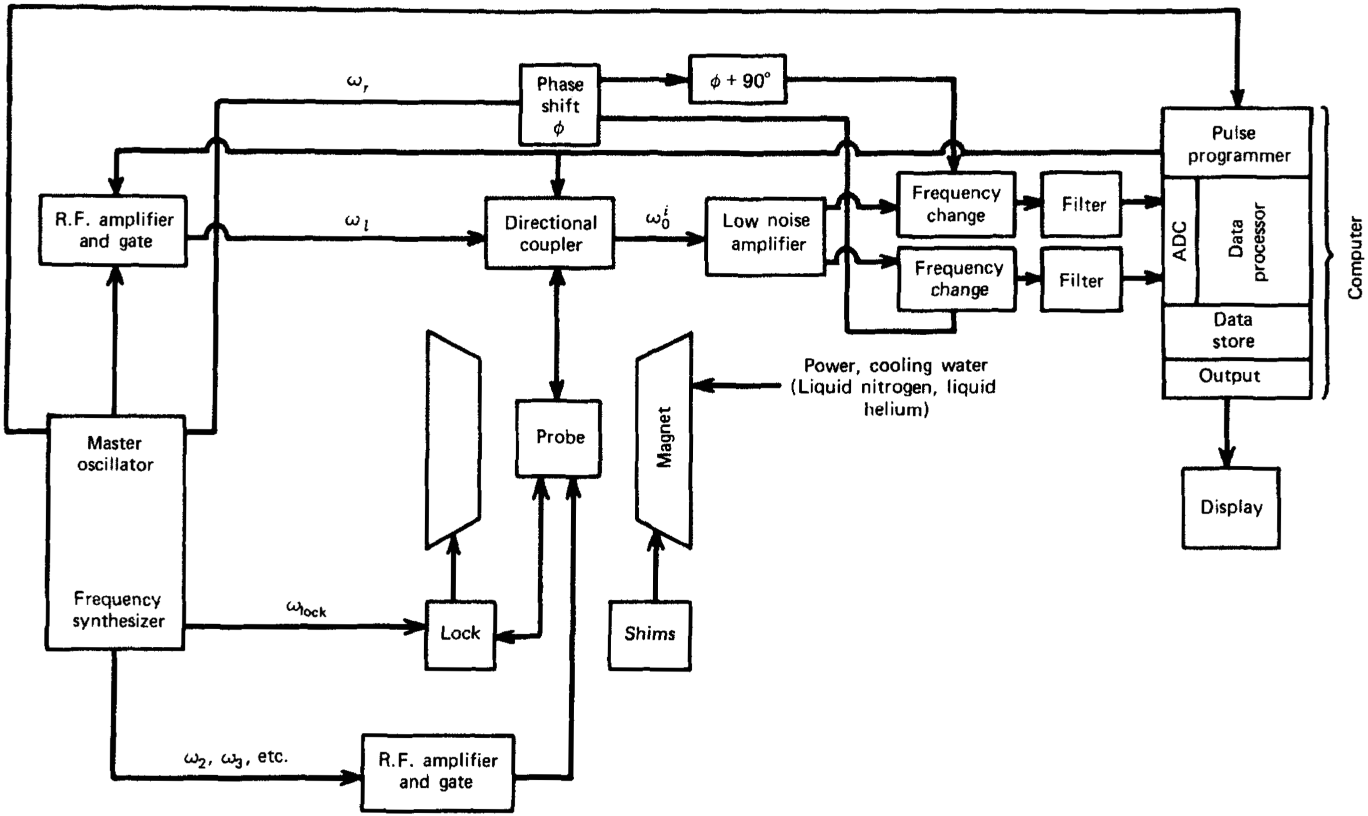
ω_r
Phase shift ϕ
$\phi + 90°$
Pulse programmer
R.F. amplifier and gate
ω_1
Directional coupler
ω_0^i
Low noise amplifier
Frequency change
Frequency change
Filter
Filter
ADC
Data processor
Data store
Output
Computer
Power, cooling water (Liquid nitrogen, liquid helium)
Probe
Magnet
Display
Master oscillator
Frequency synthesizer
ω_{lock}
Lock
Shims
ω_2, ω_3, etc.
R.F. amplifier and gate

Figure 8. A schematic diagram of a modern high resolution pulsed spectrometer. All the frequencies and pulses are derived from a master oscillator. The magnetic field homogeneity is improved by a system of shims, and the field is stabilized with an NMR resonance of frequency ω_{lock}. The observed signals of frequency $\omega_0{}^i$ are stimulated by a pulse of frequency ω_1. The large pulses are separated from the weak signals at $\omega_0{}^i$ by a directional device involving diodes (25). The signals are amplified, the frequency is changed to $\omega_0{}^i - \omega_r$, and if two frequency changers are used, the sign of $\omega_0{}^i - \omega_r$ may be determined. This duplication, involving reference frequencies 90° out of phase with respect to each other, is known as quadrature detection. The signals are then filtered and added into a computer for data processing.

Apart from obvious differences between superconducting magnets and electromagnets, such as the maximum field attainable and the very different maintenance requirements, another factor affects performance. In electromagnets the sample tube is inserted at right angles to the field direction, whereas in superconducting solenoid magnets the sample is inserted parallel to the field direction. This makes a difference in the type of tuned circuit that can be used, since B_1 must be produced at right angles to B_0 (see Table III and Ref. 27).

It seems likely that for biological work, superconducting magnets will become standard. There will probably be, however, two distinct types, one of relatively narrow bore, used to observe ^{1}H nuclei in small sample tubes (~0.4 ml of sample) at fields of 10 T or higher, the other of wider bore, used to observe ^{13}C, ^{31}P, and perhaps ^{15}N, ^{2}H, and ^{19}F, at around 5 T in large sample tubes (~10 ml of sample). There are several reasons for using the lower field and larger volume of sample for these nuclei (e.g., ^{31}P); (*a*) highly purified material is often unnecessary, and therefore more is available for the large tubes; more is also necessary because of lower sensitivity (Tables I and III); (*b*) there are problems in spin-decoupling ^{1}H from ^{13}C and ^{15}N at high ^{1}H resonance frequencies; (*c*) chemical shift anisotropy has been shown to be a dominant relaxation mechanism for ^{19}F, ^{31}P, and some ^{13}C resonances at very high fields—thus resolution gets worse, in some cases, on increasing B_0. [In some cases where paramagnetic ions are present ^{1}H resonances may also become broader at higher fields (28).]

An interesting variation on the magnetic field theme is related to the recent use of NMR to produce images of a sample (29). One aim of this work is to have magnets big enough to enclose a person. Various field gradients are generated across the sample, and this eventually allows a map to be made of the NMR signals from various regions of the sample. The technique has been named *zeugmatography* (29).

2. Excitation of the Resonances by B_1

Consider the excitation in terms of the Bloch equations [4], and see also Appendix C. The applied field B_1 is considered to lie along the x'-axis. (Note that B_1 can be made to lie along y', $-x'$, or $-y'$ by changing the phase of the transmitter frequency by 90°, 180°, or 270°; see Figure 4.) If the frequency of B_1 (ω_1) equals ω_0, the effective field along z vanishes in the rotating frame and B_1 induces a rotation of the magnetization about the x'-axis at a frequency $\omega = \gamma B_1$ (from [1].) Thus after a time t_p, the magnetization precesses through an angle $\theta = \gamma B_1 t_p$. When $\theta = \pi/2$, the application of B_1 for a time t_p is called a *90° pulse*. Pulses denoted 180°, 270°, and so on, then have the obvious meaning. Often θ is known as the flip angle.

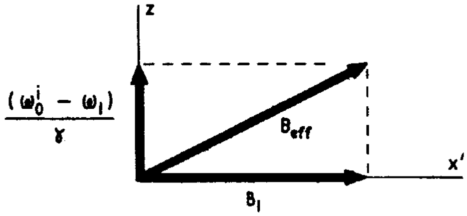

Figure 9. Definition of B_{eff}. In the rotating frame (frequency ω_1) the apparent field along z is $(\omega_0{}^i - \omega_1)/\gamma$ for a nucleus i of resonant frequency $\omega_0{}^i$ and magnetogyric ratio γ; B_1 is applied along x', but B_{eff} is equal to B_1 only when $\omega_0{}^i = \omega_1$.

If $\omega_1 \neq \omega_0$, then on application of B_1, the effective field B_{eff}, experienced by the nucleus may be different from B_1 (Figure 9). If $(\omega_1 - \omega_0) \gg B_1$, then B_1 will have very little effect on the resonance of frequency ω_0, but B_1 will have a large effect when $\omega_1 \simeq \omega_0$. In other words, the influence of B_1 is finite and is related to the magnitude of B_1. The effect of B_1 is also related to the time for which B_1 is applied, by a Fourier transform relationship (see Appendix C). This introduces the idea of *selective* and *nonselective* pulses. A wide spectrum is affected by a short, large magnitude pulse (i.e., nonselective) or a small region is affected by a long, low magnitude pulse (i.e., selective). If a 90° pulse has a length t_p, the region affected is of the order of $1/t_p$ Hz (see Appendix C).

If B_1 is applied for a long time to the sample, and if γB_1 is much larger than the linewidth of the observed resonance, the magnetization M_0 not only rotates around B_{eff} at frequency B_1 but also decays toward a new equilibrium value at a rate $\frac{1}{2}(1/T_1 + 1/T_2)$ (30). The new value is $M_z = M_0/(1 + \gamma^2 B_1{}^2 T_1 T_2)$. These relationships can be obtained by solution of the Bloch equations. [If B_1 is inhomogeneous, the decay rate toward the new value may be much faster than indicated here (31)]. Note that if $\gamma^2 B_1{}^2 T_1 T_2 \gg 1$ the magnetization tends to zero. This phenomenon, known as *saturation*, means that there is always an *optimum* in the excitation process, involving a compromise between inducing a maximum signal and avoiding saturation. In a simple pulse experiment, for example, this compromise is achieved by repetitive pulses separated by less than T_1 and with a pulse angle less than 90°.

There are many possible ways of exciting an NMR spectrum and some of these are indicated in Table IV. In the *continuous wave* method a small B_1 field is applied to the sample and the frequency is swept over the spectral region very slowly so that an approximate steady state is achieved, with M_z never being tipped far from the z-direction. This process is very slow, and for weak samples with many lines the rate at which information can be collected is slow. If the sweep rate is increased to improve the data collection rate, each resonance "rings" at its resonance frequency after being excited by the B_1 field

TABLE IV

Some Methods of Exciting and Detecting NMR Signals

		Application of B_1 field				
Method	Reference	Frequency source	Timescale	Magnitude of B_1	Shape of excitation function	Collection efficiency
Continuous wave	9	Slow linear sweep between ω_s and ω_f	Continuous application	Small	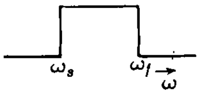	Poor
Time-sharing	40	Slow sweep between ω_s and ω_f	Continuous train of short pulses	Intermediate		Poor
Correlation spectroscopy	32	Fast sweep between ω_s and ω_f	Continuous repetitive application	Intermediate	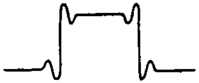	Good
Stochastic resonance	33	Single frequency, but effectively spread over defined region	Continuous repetitive application in tailored pulse sequence	Intermediate	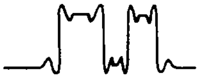	Good
Pulsed or Fourier transform NMR	36	Single frequency	Short pulse	High	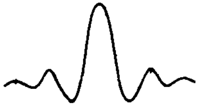	Good

and, since ω_1 is varying continuously, a very complex spectrum results because of interference between the resonance frequency and ω_1. This spectrum can, however, be interpreted with sophisticated data processing that involves correlating the spectrum with another spectrum having a known response function (see Appendix A). This technique, developed by Dadok (32), is known as *correlation spectroscopy*. It has some advantages, especially in the presence of large solvent peaks, since these peaks need not be excited. One other method that deserves mention includes the use of pseudorandom pulses to generate a defined excitation spectrum (33). The approach is referred to as *stochastic resonance*; detection is not particularly easy, and the method lacks the versatility of simple pulse methods. However the excitation spectrum is relatively precise, and this part of the method could be very useful in double resonance work (34).

The method we concentrate on in this chapter is the short pulse or Fourier transform method (35, 36; see Ref. 37 for a simple introduction). This method is readily available commercially, it is very versatile, and it is the only method suitable for measuring some relaxation rates. The only real difficulty is the shape of the excitation function, which is not well defined, and this means that it may be difficult to excite selectively part of a spectrum. However the short pulse method is likely to remain the method of choice for most workers in this field.

3. Detection of the Signals

The signals induced in the x,y-plane by the various excitation methods are detected by means of a tuned coil (the probe) containing the sample. The signals are usually very small, and very sophisticated methods must be used to obtain the maximum possible signal-to-noise ratio.* Modern methods all involve amplification at the resonance frequency, changing the frequency to a lower one, and some kind of signal processing in a computer. We again concentrate on pulse methods, but most of the discussion is quite general.

In a well-constructed spectrometer, the noise comes entirely from the probe and the first stage of amplification. Modern amplifiers, however, can be made to be very efficient, and the noise introduced at this stage should be 20% or less. The noise therefore arises almost entirely from the thermal motion of the electrons in the conductor of the tuned circuit of the probe. The geometry of the probe coil is important, both for the homogeneity of the B_1 excitation and the efficiency of coupling between the sample and the coil (see Table III).

---

* The *signal-to-noise ratio* of a resonance is defined, by convention, as the ratio of the maximum signal to the peak-to-peak noise multiplied by 2.5. Various standard samples are used in specifications; for example, the quartet of 1% ethyl benzene is used as the standard in ^{1}H NMR. The optimum filter is used; that is, the free induction decay is convoluted with an exponential with the same decay rate as the signal of interest.

The frequency changing is achieved by mixing the detected signals of frequency $\omega_0{}^i$ with a reference frequency ω_r. This results in two sets of frequencies being generated, one at $\omega_0{}^i - \omega_r$, the other at $\omega_0{}^i + \omega_r$. The higher frequencies are normally rejected by filtering. This frequency changing process can lead to distortions, since electronic multiplication is not always straightforward. Moreover, some information is lost because it is not possible, in a simple mixing process, to tell the sign of $\omega_0{}^i - \omega_r$. Thus if ω_r comes in the middle of spread of $\omega_0{}^i$ values, the inability to determine the sign results in a "folded" spectrum. This may be overcome by setting ω_r to less than all the $\omega_0{}^i$ values, but this is inefficient because the bandwidth must be set too high. Another method of overcoming this problem involves the use of *quadrature detection* (26,38). This approach entails duplication of the detector after frequency changing, with signals 90° out of phase with respect to each other. These two components are added into the computer simultaneously but separately, and it is possible to determine the sign of $\omega_0{}^i - \omega_r$, which is equivalent to knowing the direction of rotation (see Figure 8). The only difficulty presented by this method is that the two channels must be accurately 90° out of phase with respect to each other. Methods have been devised, however, that allow this to be done (26), and quadrature detection will no doubt become a standard feature in sophisticated instruments.

Consider the response to a 90° pulse which is, from a solution of [4], of the form $f(t) = \exp(-t/T_2) \cos \omega_0{}^i t$. This transient signal, normally called a free induction decay, is detected; its frequency is changed to $\omega_0{}^i - \omega_r$, and it is amplified and stored in a computer. The normal procedure is to add up large numbers of these transient signals, each lasting about 1 sec. The effect of this is to improve the signal-to-noise ratio, because although the signals add up directly, the noise only adds up as the square root of the number of signals. This process is known as *signal averaging* and gives an improvement in signal-to-noise ratio proportional to the square root of the accumulation time.

The averaged signals are then processed in the computer. In a complex spectrum with many different kinds of nucleus, each type having a characteristic value of $\omega_0{}^i$ and T_2, the transient response is difficult to interpret, and the signal is *Fourier transformed* (Appendix A) to give a frequency domain spectrum. Before Fourier transformation, it is customary to multiply the time domain signal with a decreasing exponential, which increases the linewidth in the frequency domain by a known amount (Appendix A) and improves the signal-to-noise ratio. Alternatively, the data can be multiplied by an increasing exponential, which decreases the linewidth and signal-to-noise ratio. These processes are sometimes called *convolution* and *deconvolution*, respectively (36). The Fourier transformation produces a sine and cosine transform of the information, or real and imaginary parts as they are often called (see Appendix A). Suitable mixing of these two transforms allows the *phase* of the spectrum to be adjusted (Section II.4.D). This usually involves a frequency-independent and a frequency-dependent adjustment.

The computer itself introduces some limitations. The incoming signal(s) must be digitized in an analog-to-digital converter (ADC). These devices are specified by a resolution, that is, the number of discrete levels into which the signal is divided, and the rate at which the conversion can be performed. Obviously the better the resolution, the better the signal is represented, but then the total number of scans that can be accumulated in the computer before overflow may be limited. For example, if the ADC has a 12-bit resolution (2^{12} divisions), then for a 16-bit computer word length, only 2^4 scans can be accumulated if the incoming signal is coherent. The rate of conversion must be at least twice as fast as the frequency of the incoming signal if the signal is to be properly represented. If the signal is sampled at less than this rate, the phenomenon known as *aliasing* occurs; that is, the signal has an apparent frequency, lower than the real one. In addition to ADC problems, some resolution is lost in the Fourier transformation because of the algorithm used, but this can be recovered by doubling the size of the data block using zeros, before transformation. The computer must also have a large data store (up to 32K words) to represent adequately some very detailed spectra. Some other factors related to the computer, such as noise introduced by round-off errors, have been discussed by Cooper (39).

4. Longitudinal Relaxation

The relaxation along the z-direction is readily measured using pulsed NMR, but several possible methods may be used. Some of these have been reviewed by Levy and Peat (41), and four are summarized in Table V. The simplest

TABLE V

Some Methods for Measuring Longitudinal Relaxation Times, T_1

	Method	Pulse sequence[a]	Reference
A.	Inversion recovery (I)	$(180°\text{-}\tau\text{-}90\text{-AT-D})_n$	42
B.	Inversion recovery (II)	$(180°\text{-}\tau\text{-}90\text{-AT-D-}90\text{-AT-D})_n$	43
C.	Progressive saturation	$(90°\text{-}\tau\text{-AT})_n$	44
D.	Saturation recovery	$(90°\text{-HS-}\tau\text{-}90°\text{-AT-HS})_n$	45

[a] Symbols: τ, a variable pulse delay; n, the number of scans performed at each τ value; AT, the time taken for the data acquisition; D, a delay to allow the system to return to equilibrium; HS, a pulse that degrades the homogeneity of the magnet, thus causing a dephasing of any components in the x,y-plane.

method is the inversion recovery method, where a 180° pulse is applied to the system, thus causing the magnetization to invert and become $-M_0$. The recovery back to $+M_0$ is monitored by a series of 90° pulses at various time intervals (τ). The modification of this method involving the measurement of $M_0 - M(\tau)$ (method B) is probably the most accurate means of measuring T_1, although the simple inversion recovery is also good for most purposes. If T_1 is very long, the other two methods have some advantages, but these are, in our experience, more prone to systematic errors. When there are imperfections in the 180° pulse, components are induced in the x,y-plane. These components can interfere with the signal after the monitoring pulse, causing apparent phase anomalies in the spectrum at short τ values. These anomalies can be reduced by switching the phase of the transmitter or by using a pulse to spoil the homogeneity (41).

In addition to the methods just outlined and listed in Table V, various other experimental methods can be used to obtain useful information about the z-magnetization (17,46). To illustrate some of these interesting approaches, consider the relaxation rates predicted by solution of the dipole-dipole interaction [6] under various experimental conditions. For simplicity, assume that $\rho_I = \rho_S = \rho$.

CASE A

A nonselective 180° pulse which affects the I and S spins equally. In this case $I_z \simeq S_z$ and the recovery is given by

$$\frac{dI_z}{dt} = -(\rho + \sigma)(I_z - I_0)$$

which is an exponential with rate constant $\rho + \sigma$.

CASE B

A selective pulse on the I spin only. The S_z magnetization is initially at equilibrium (S_0), but as I_z recovers, S_z is reduced because of the σ term in [6]. The relaxation of I_z is nonexponential, but suitable corrections can sometimes be made (17). In the homonuclear case, where I_z and S_z can be observed simultaeously with a nonselective monitoring pulse, the complex behavior of I_z and S_z can be readily analyzed by taking sums and differences of S_z and I_z (47). For example, $d(S_z + I_z)/dt = -(\rho + \sigma)[(I_z + S_z) - (I_0 + S_0)]$ represents an exponential with rate constant $\rho + \sigma$. The difference $[d(S_z - I_z)/dt]$ is also exponential with rate constant $\rho - \sigma$. (This type of analysis can also be applied to [17], which represent the "slow chemical exchange" limit, see Section V.2 and Figure 10).